Molecular Imaging
Volume 17: 1-9

DOI: 10.1177/1536012118811741
journals.sagepub.com/home/mix
SAGE

Scatter Artifact with Ga-68-PSMA-11 PET: Severity Reduced With Furosemide Diuresis and Improved Scatter Correction

Courtney Lawhn-Heath, MD[1], Robert R. Flavell, MD, PhD[1], David E. Korenchan, PhD[1], Timothy Deller, MSEE[2], Spencer Lake, MD[1], Peter R. Carroll, MD, MPH[3], and Thomas A. Hope, MD[1,4]

Abstract

Purpose: To assess the utility of furosemide diuresis and the role of an improved scatter correction algorithm in reducing scatter artifact severity on Ga-68- Prostate-specific membrane antigen (PSMA)-11 positron emission tomography (PET).

Materials and Methods: A total of 139 patients underwent Ga-68-PSMA-11 PET imaging for prostate cancer: 47 non-time-of-flight (non-TOF) PET/computed tomography, 51 PET/magnetic resonance imaging (MRI) using the standard TOF scatter correction algorithm, and 41 PET/MRI using an improved TOF scatter correction algorithm. Whole-body PET acquisitions were subdivided into 3 regions: around kidneys; between kidneys and bladder; and around bladder. The images were reviewed, and scatter artifact severity was rated using a Likert-type scale.

Results: The worst scatter occurred when using non-TOF scatter correction without furosemide, where 42.1% of patients demonstrated severe scatter artifacts in 1 or more regions. Improved TOF scatter correction resulted in the smallest percentage of studies with severe scatter (6.5%). Scatter ratings by region were lowest using improved TOF scatter correction. Furosemide reduced mean scatter severity when using non-TOF and standard TOF.

Conclusions: Both furosemide and scatter correction algorithm play a role in reducing scatter in PSMA PET. Improved TOF scatter correction resulted in the lowest scatter severity.

Keywords

cancer detection imaging, clinical translational molecular imaging, PET, cancer imaging, PSMA

Introduction

Prostate-specific membrane antigen (PSMA) positron emission tomography (PET) using Ga-68-PSMA-11 is a highly sensitive and specific imaging technique for prostate cancer.[1-4] The Ga-68-PSMA-11 demonstrates a high target-to-background ratio and prominent renal excretion.[5] Furthermore, PSMA inhibitors such as Ga-68-PSMA-11 are retained in the kidney cortex. This combination of characteristics leads to high levels of activity in the urinary system (kidneys, ureters, and bladder), which may limit sensitivity for detection of lower levels of abnormal activity in surrounding structures, including retroperitoneal and pelvic lymph nodes, which are common sites of metastatic prostate cancer. Similarly, scatter correction algorithms used in PET image reconstruction can result in photopenic regions around the urinary system, potentially lowering sensitivity or interfering with an accurate image interpretation.[1] The severity of this artifact varies with acquisition method, with time-of-flight (TOF) acquisition generally considered superior to earlier non-TOF methods.[6,7]

[1] Department of Radiology and Biomedical Imaging, University of California–San Francisco, San Francisco, CA, USA
[2] GE Healthcare, Waukesha, WI, USA
[3] Department of Urology, University of California–San Francisco, San Francisco, CA, USA
[4] Department of Radiology, San Francisco VA Medical Center, San Francisco, CA, USA

Submitted: 02/02/2018. Revised: 05/10/2018. Accepted: 08/10/2018.

Corresponding Author:
Courtney Lawhn-Heath, University of California–San Francisco, 505 Parnassus Avenue, San Francisco, CA 94143, USA.
Email: courtney.lawhnheath@ucsf.edu

Furosemide (Lasix) administration has demonstrated efficacy in improving overall image quality and lesion detectability in PET using renally excreted radiotracers, including Ga-68-PSMA-11.[5,8,9] A recent study using furosemide with Ga-68-PSMA-11 demonstrated improved image quality and lesion detection with the use of delayed furosemide administration after radiotracer administration.[8] However, scatter correction artifact in Ga-68-PSMA-11 PET imaging has not yet been evaluated.

The aim of this study was to assess the usefulness of furosemide diuresis and the role of an improved scatter correction algorithm in reducing scatter artifact severity.

Materials and Methods

Setting and Participant Selection

A subset of patients enrolled in a prospective trial of Ga-68-PSMA-11 (NCT02611882) evaluating Ga-68-PSMA-11 for the detection of prostate cancer were retrospectively analyzed as part of this study. All patients provided informed consent, and these studies were approved by the local institution review board. The study included patients with newly diagnosed or biochemically recurrent prostate cancer who underwent a whole-body Ga-68-PSMA-11 PET using either PET/computed tomography (CT; Discovery VCT, GE Healthcare, Waukesha, Wisconsin) or PET/ magnetic resonance imaging (MRI; Signa 3.0 T TOF PET/MRI; GE Healthcare) at University of California–San Francisco.

Imaging Protocols and Image Reconstruction

Ga-68-PSMA-11 was prepared as described previously using an ITG germanium-gallium generator and an iQs fluidic labeling module (ITG, Gärching/Munich, Germany).[10] 111-259 MBq (3-7 mCi) of Ga-68-PSMA-11 was injected intravenously. In a subset of cases, a dose of 20 mg of furosemide was injected together with the administration of the radiotracer. Reasons for not administering furosemide included allergy, hypotension, patient refusal, and technical/nursing error. In all cases, patients were encouraged to void prior to imaging. Patients were scanned with PET/CT (Discovery VCT, GE Healthcare) or PET/MRI (3.0 T TOF Signa PET/MRI; GE Healthcare). On average, PET imaging began 68.4 minutes (range 45-162, standard deviation [SD]16.1) after injection. For PET/CT, the pelvis to vertex was imaged using a 5-minute acquisition per bed position from the pelvis through the mid-abdomen and 3-minute acquisitions from the upper abdomen to the vertex. Iodinated contrast was administered to all patients, unless contraindicated. A postcontrast diagnostic CT was then obtained and used for attenuation correction (mA = 240, kV = 120, slice thickness = 2 mm). PET data were reconstructed using iterative reconstruction with 4 iterations and 14 subsets and a matrix size of 168 × 168. The PET transaxial field of view was 620 mm, and axial slice thickness was 5.0 mm.

For PET/MRI, a pelvis and abdomen bed position was imaged using an 8-minute acquisition. The PET data were reconstructed using TOF, Ordered Subset Expectation Maximization (OSEM) using 2 iterations and 28 subsets and a matrix size of 256 × 256, with a 600 × 250 mm field of view and a 2.8 mm slice thickness. A dynamic contrast-enhanced sequence was acquired of the pelvis after the administration of gadolinium, followed by T2-weighted, diffusion-weighted, and a post-gadolinium delayed axial T1-weighted imaging. For the whole-body acquisition, PET data were acquired for 3 minutes at each bed position with axial T1- and T2-weighted sequences in the coronal and axial plane. Attenuation correction was performed as described previously[11] with a standard 2-point Dixon acquisition converted into an attenuation map.

On PET/CT, patients were imaged with the arms up if tolerated. If a patient was unable to tolerate this positioning due to pain or other discomfort, the patient was imaged with 1 or both arms down. On PET/MRI, patient's arms are imaged with their arms down. This is standard on all PET/MRI studies, as the arms do not create streak artifact that can be limiting in PET/CT. It is more comfortable for the patient and does not interfere with MR image quality.

Scatter Correction Algorithm

Standard scatter correction algorithms were developed for F-18 tracers and tend to overestimate scatter in areas of high uptake using Ga-68-labeled tracers such as PSMA and somatostatin receptor agents due to higher target to background ratios. Developing an improved algorithm involved modifying multiple parameters that were originally developed in the setting of fluorodeoxyglucose-PET.[12] For more accurate scatter estimation using Ga-68 PET, the number of axial subsamples was increased. To compensate for the resultant increased computational load, the image grid was downsampled in the coronal and sagittal planes. Standard scatter tails were modified by a factor determined by a least squares fit for each plane and then axially smoothed. A factor taking into account the prompt γ associated with Ga-68 was also added to the model. Standard scatter correction algorithms do not incorporate this factor because 18-F does not have a prompt γ phenomenon. This resultant improved scatter correction algorithm has recently been described in detail.[13] Figure 1 shows the same patient scanned using standard TOF (A-C) and improved TOF (D-F) scatter correction.

Imaging Data Collection and Analysis

The whole-body PET images for each study were reviewed by 2 readers (CL and SL) on a PACS workstation (Agfa Healthcare, Mortsel, Belgium). The PET images were evaluated for the presence of scatter artifact within the abdomen/pelvis at 3 levels: kidneys, between kidneys and bladder, and bladder. Scatter artifact severity at each level was rated using a Likert-type scale as follows: 1 = none; 2 = mild, involving a small to medium region, unlikely to hinder diagnosis; 3 = moderate, involving a large region; 4 = severe, dense artifact over a small to medium region, likely to obscure small lesions;

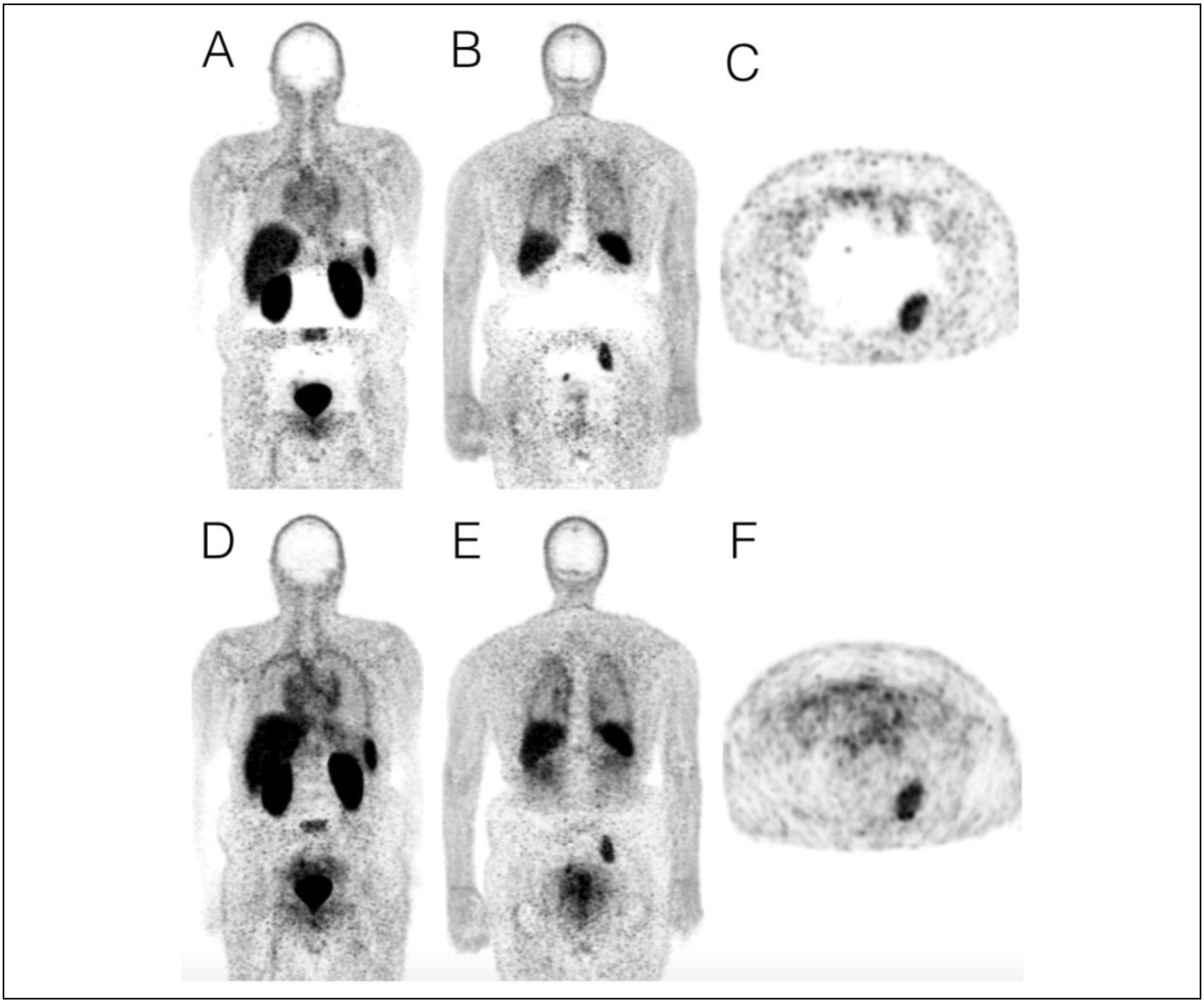

Figure 1. Coronal (A and B, D and E) and axial (C and F) Ga-68-PSMA-11 positron emission tomography (PET) images of the same patient with standard time-of-flight (TOF) scatter correction (A-C) and improved TOF scatter correction (D-F), demonstrating marked reduction in scatter artifact with improved TOF.

and 5 = very severe, dense artifact over a large region, likely to obscure large lesions (Figure 2). The PET images were scaled to accentuate the artifact seen. The ratings from both reviewers were averaged to arrive at a final mean artifact severity rating per level. On a dedicated workstation using Advanced Workstation for Diagnostic Imaging (GE Healthcare), Maximum Standardized Uptake Value (SUVmax) was measured at the kidneys, bladder, and background using volumes of interest measuring at least 20 mm in diameter. Background SUVmax was measured at the right thigh.

A retrospective chart review was performed in an electronic medical record system, and demographic data were collected for each study, including patient age, height, weight, and Prostate-Specific Antigen (PSA) level; imaging modality (PET/CT vs. PET/MRI); time and dose of radiotracer administration; time and dose of furosemide administration (if given); and start time of PET acquisition.

Statistical Analysis

Interrater reliability was evaluated using Cohen κ. Statistical analysis was performed using R version 3.3.3. Differences in mean scatter severity by body mass index (BMI) and by scan delay time were compared using *t* tests. Standard deviation and error as well as *t* tests were calculated, and figures were constructed using Microsoft Excel 2011 for Mac. Linear regression between mean scatter artifact score and maximum SUV was performed in MATLAB (Mathworks, Natick, Massachusetts). Statistically significant correlations were identified using a 2-tailed nonparametric Spearman rank correlation coefficient test.

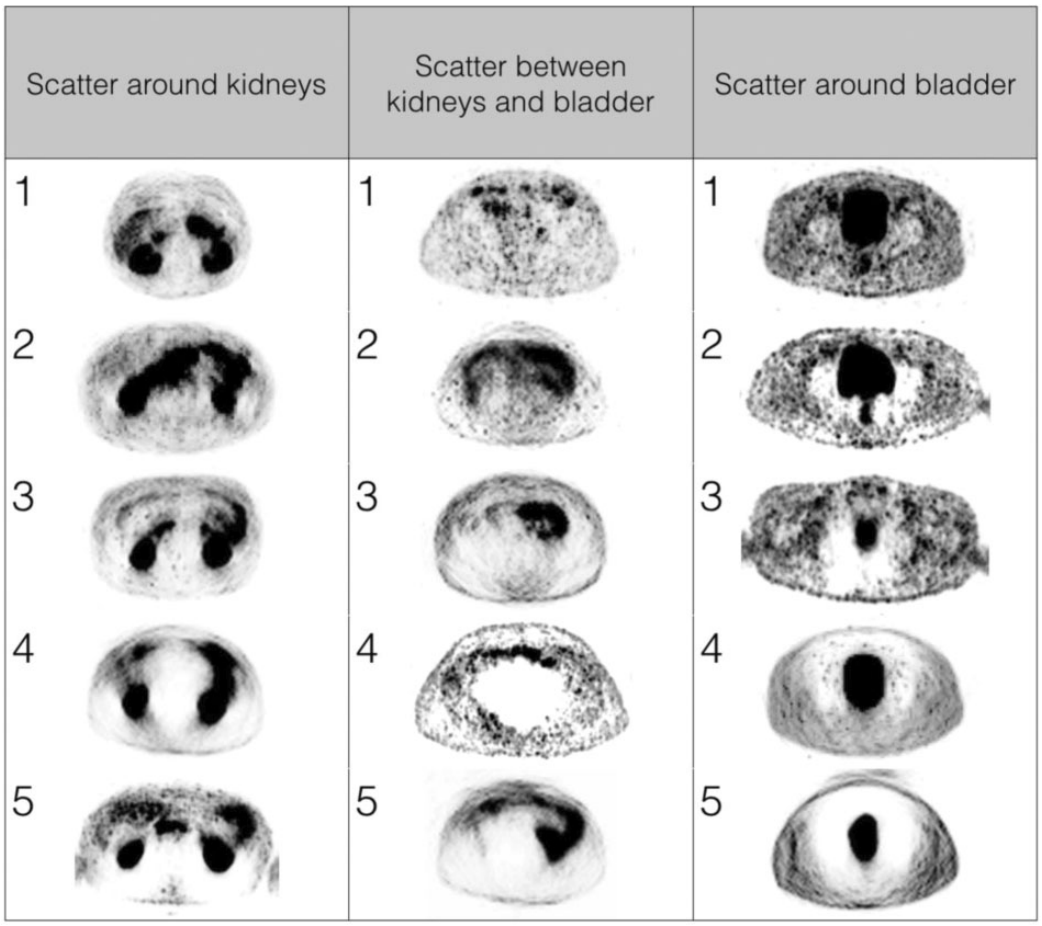

Figure 2. Scatter rating examples. Scatter artifact severity at each level was rated using a Likert-type scale as follows: 1 - none; 2 - mild, involving a small to medium region, unlikely to hinder diagnosis; 3 - moderate, involving a large region; 4 - severe, dense artifact over a small to medium region, likely to obscure small lesions; and 5 - very severe, dense artifact over a large region, likely to obscure large lesions.

Results

A total of 139 patients were evaluated. Forty-seven patients underwent non-TOF PET/CT of which 28 received furosemide; 51 patients underwent PET/MRI with a standard TOF scatter correction algorithm of which 36 received furosemide; and 41 patients underwent PET/MRI with an improved TOF scatter correction algorithm of which 34 received furosemide (Table 1). Of note, the time between radiotracer administration and scanning was similar between non-TOF PET/CT (63.1 minutes, SD 11.2 minutes) and standard TOF PET/MRI (62.1 minutes, SD 5.9 minutes) but was longer with improved TOF PET/MRI (82.8 minutes, SD 20.5 min).

Subjective Scatter Ratings

Interrater agreement was moderate at all regions evaluated (κvalues: kidneys = 0.44, between kidneys and bladder = 0.49, and bladder = 0.49). Score distributions of the individual raters are shown in Figure 3. The worst scatter artifact occurred when using non-TOF scatter correction without furosemide, where 42.1% of studies demonstrated severe[4] or very severe[5] scatter artifacts in 1 or more regions, compared to 21.4% with furosemide (Figure 4A). Improved TOF resulted in the lowest percentage of studies with severe scatter at 1 or more regions, 0% to 6.2% compared to 22.2% to 33.3% with standard TOF and 21.4% to 42.1% with non-TOF (Figure 4A). Improved TOF also resulted in the lowest percentage of studies with severe scatter at each evaluated region (Figure 4B-D). Mean scatter severity ratings were lowest in all 3 evaluated regions with improved TOF scatter correction, which resulted in very little scatter artifact overall (Figure 5A-C). Within a given scatter correction algorithm, furosemide administration resulted in lower mean scatter ratings with non-TOF and standard TOF but not with improved TOF (Figure 5A-C). Taking all acquisitions as a whole, longer scan delay times (90+ minutes) were associated with a small but statistically significant improvement in mean scatter severity ratings compared to shorter delay times (<90 minutes; mean scatter ratings of 1.6 and 1.3, respectively; $P < .01$; Table 2). In addition, BMI of 30+ (obese) resulted in a small but statistically significant increase in scatter artifact compared to patients with BMI <30 (1.8 and 1.6, respectively; $P < .01$; Table 3).

Table 1. Characteristics of the Study Population.[a]

	Non-TOF	Standard TOF	Improved TOF
# Participants, total	47	51	41
−furosemide	19	15	7
+ furosemide	28	36	34
Age, years, total (SD)	67.9 (8.5)	67.7 (7.0)	68.4 (6.9)
−furosemide	67.3 (7.6)	65.7 (7.4)	71.7 (5.3)
+ furosemide	68.2 (9.2)	68.6 (6.7)	68.4 (7.1)
Body mass index (BMI), total (SD)	27.3 (4.6)	26.1 (3.0)	27.3 (4.2)
−furosemide	27.7 (4.6)	25.5 (2.4)	26.1 (3.6)
+ furosemide	27.1 (4.7)	26.4 (3.2)	27.6 (4.3)
Height, cm, total (SD)	179.9 (7.5)	177.7 (6.1)	177.5 (7.1)
−furosemide	179.4 (8.5)	176.9 (7.2)	180.2 (8.2)
+ furosemide	180.2 (6.7)	178.1 (5.6)	176.9 (6.8)
Weight, kg, total (SD)	88.5 (16.1)	82.4 (10.7)	86.3 (14.4)
−furosemide	89.3 (14.6)	79.5 (7.0)	84.8 (14.4)
+ furosemide	88.2 (17.4)	83.7 (11.8)	86.1 (14.6)
PSA, ng/mL, total (SD)	12.0 (16.1)	9.8 (13.1)	11.0 (16.8)
−furosemide	13.6 (9.9)	9.8 (11.5)	13.9 (17.9)
+ furosemide	8.4 (19.1)	11.7 (13.8)	10.6 (16.8)
Tracer dose, mCi, total (SD)	5.6 (1.2)	5.3 (0.8)	6.4 (0.9)
−furosemide	5.3 (0.6)	5.4 (0.6)	6.2 (0.8)
+ furosemide	6.1 (1.4)	5.1 (0.9)	6.4 (0.9)
Scan delay, minutes, total (SD)	63 (11.3)	62 (5.9)	82.8 (20.5)
−furosemide	61 (6.2)	64 (5.0)	80 (7.2)
+ furosemide	65 (13.6)	60 (6.0)	80 (22.4)

Abbreviations: SD, standard deviation; TOF, time-of-flight.
[a]Continuous variables are expressed as mean (standard deviation).

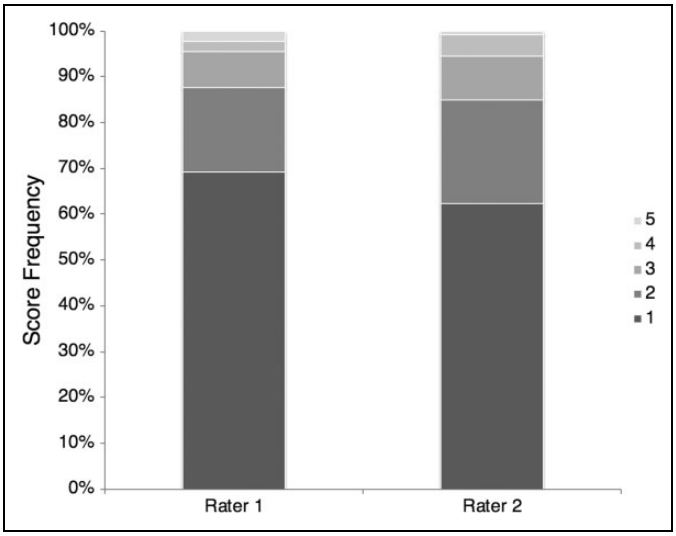

Figure 3. Scatter score distribution by rater for all 3 evaluated regions combined.

Renal and Bladder Activity on Ga-68-PSMA PET

Overall, higher bladder SUVmax and similar renal SUVmax were seen on both standard and improved TOF scatter algorithms compared to non-TOF (Figure 6A-C), although mean scatter severity was lower than on non-TOF. Administering furosemide was associated with lower renal and bladder SUVmax on non-TOF and lower bladder SUVmax on standard TOF (Figure 6A and B) but was not associated with a notable difference in SUVmax on improved TOF or at the kidneys on standard TOF (Figure 6B and C). Regression analysis demonstrated a statistically significant positive correlation between SUVmax and scatter severity rating at the levels of the kidneys (Supplemental Figure 1) for non-TOF imaging only ($P < .002$) but no other significant correlation between SUVmax and scatter severity.

Discussion

Scatter artifact, also known as halo artifact, washout artifact, or photopenic artifact, is a common occurrence with Ga-68-PSMA PET and may interfere with lesion detectability.[14-19] In this study, we evaluated the effect of both furosemide administration and scatter correction algorithm on subjective image quality by comparing the mean scatter severity rating of Ga-68-PSMA-11 non-TOF and TOF acquisitions. Overall scatter ratings were lowest using improved TOF scatter correction, regardless of furosemide administration and overall higher renal and bladder uptake. The TOF acquisition without improved scatter correction resulted in lower artifact than on non-TOF. The worst scatter artifact was seen with non-TOF, for which furosemide administration demonstrated a reduction in scatter severity in all 3 evaluated regions.

For non-TOF and standard TOF scatter correction algorithms, the results of our study agree with previous literature that furosemide diuresis is helpful in improving image quality.[8] In our study, furosemide administration did not significantly affect scatter severity when using improved scatter correction, although this may be due to a very low overall presence of scatter artifact compared to standard TOF and non-TOF. As such, our data suggest that furosemide administration is helpful with scanners using non-TOF and standard TOF scatter correction algorithms but may not be necessary when using an improved TOF algorithm.

Recent literature suggests that numerous factors appear to contribute to scatter artifact. Timing of image acquisition relative to radiotracer injection may play a role, although some studies favor early acquisition at approximately 1 hour post-injection (p.i.),[20,21] and others favor late acquisition at approximately 3 hours p.i.[18,22] The first joint European Association of Nuclear Medicine (EANM) and Society of Nuclear Medicine and Molecular Imaging (SNMMI) PSMA imaging guidelines recommend early imaging (50-100 minutes p.i.), citing advantages in both workflow practicality and residual activity of the radiotracer, given its shorter half-life.[16] In our study, although the improved TOF group was imaged later than the other groups, the time difference was much smaller than the 2-hour time difference between "early" and "late" imaging in the previously mentioned studies and is therefore unlikely to have had a significant effect on the reduction of scatter artifact observed in the improved TOF group. In addition, mean activity in the kidneys and bladder was similar between standard TOF and

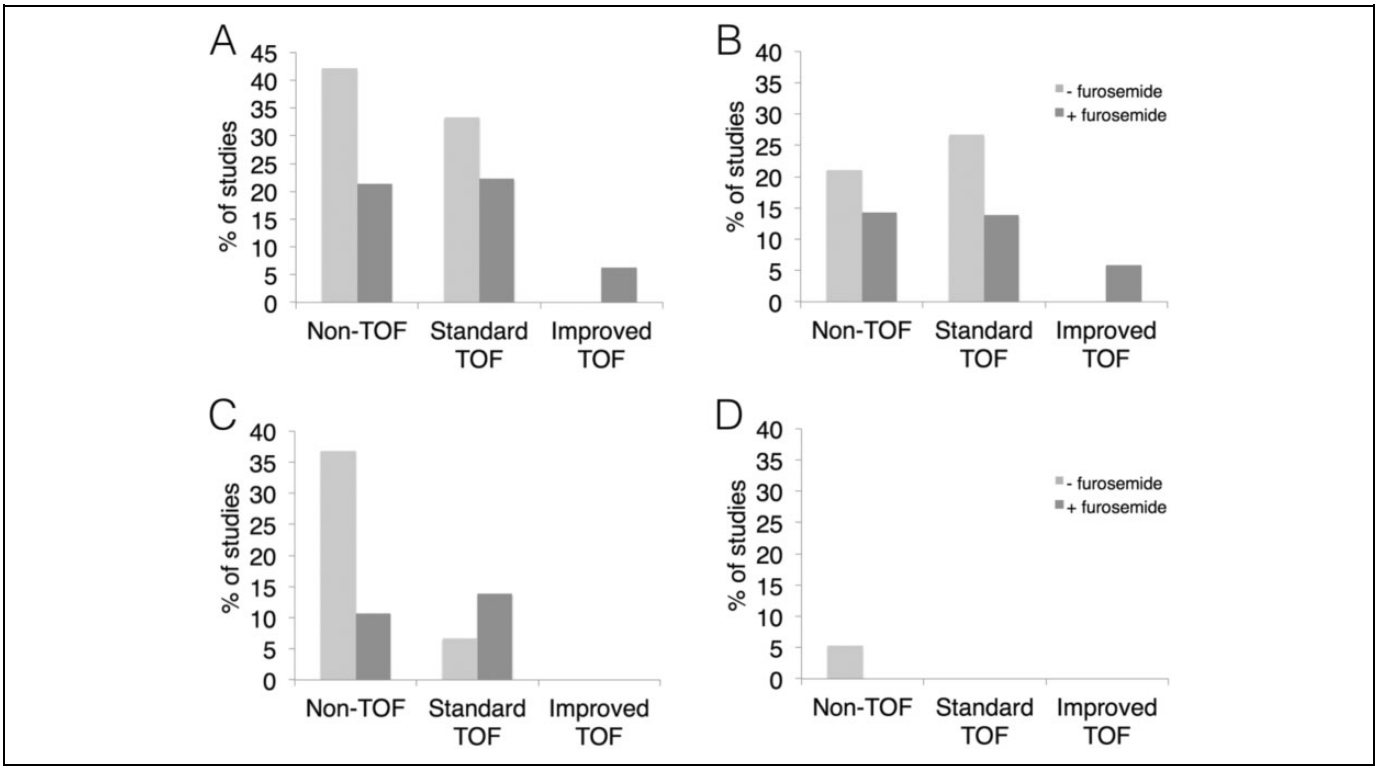

Figure 4. Percentage of studies with severe scatter artifact (mean scatter artifact rating of 4 [severe] or 5 [very severe]) broken down by region. The use of furosemide and an improved scatter algorithm resulted in a smaller percentage of studies with severe scatter artifact in any region (A), and specifically around the kidneys (B), between the kidneys and bladder (C) and around the bladder (D).

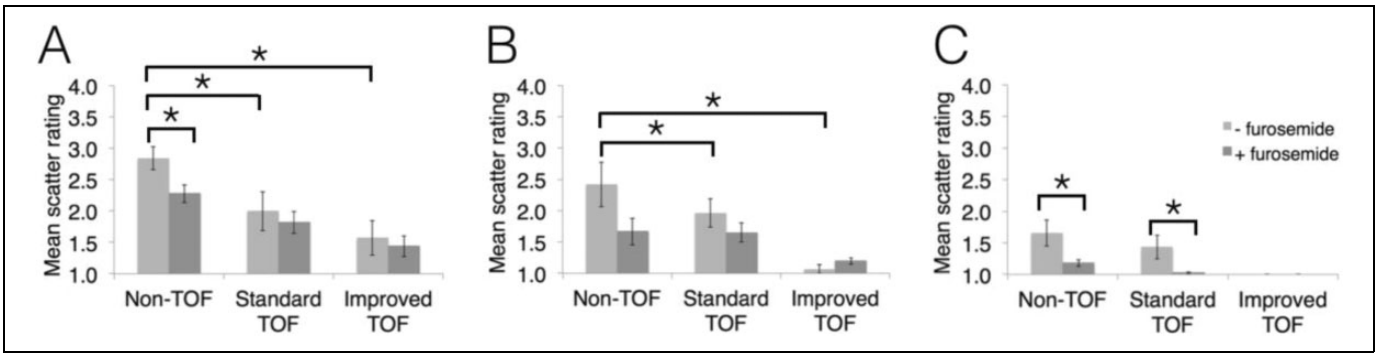

Figure 5. Mean scatter severity rating by scatter correction algorithm (non- time-of-flight [TOF], standard TOF, and improved TOF) without (−) versus with (+) furosemide administration. Improved TOF resulted in the lowest mean scatter severity ratings around the kidneys (A), between kidneys and bladder (B), and around bladder (C). Furosemide administration reduced scatter severity with non-TOF and standard TOF but not for improved TOF. (error bars = standard error. * $P < .05$).

Table 2. Mean Scatter Severity Rating and Scan Delay by region.[a]

	Scan Delay <90 min	Scan Delay 90+ min
Mean scatter severity		
Around kidneys	2.0	1.7
Between kidneys and bladder[b]	1.6	1.1
Around bladder	1.3	1.3
Overall[b]	1.6	1.3

[a]Longer delays in scanning after radiotracer administration (90+ minutes) resulted in less severe scatter than shorter delays (< 90 minutes), a difference that was statistically significant between the kidneys and bladder as well as overall ($P < .05$, indicated by an asterisk), and trended toward significance around the kidneys ($P = .067$).
[b]$P < .05$.

Table 3. Mean Scatter Severity Rating and BMI by Region.[a]

	BMI <30	BMI = 30+
Mean scatter severity		
Around kidneys[b]	1.9	2.3
Between kidneys and bladder[b]	1.5	1.9
Around bladder	1.3	1.3
Overall[b]	1.6	1.8

[a]Obese patients (BMI = 30+) had more severe scatter artifact than nonobese patients (BMI < 30), a difference that was statistically significant around the kidneys, between kidneys and bladder, and overall.
[b]$P < .05$.

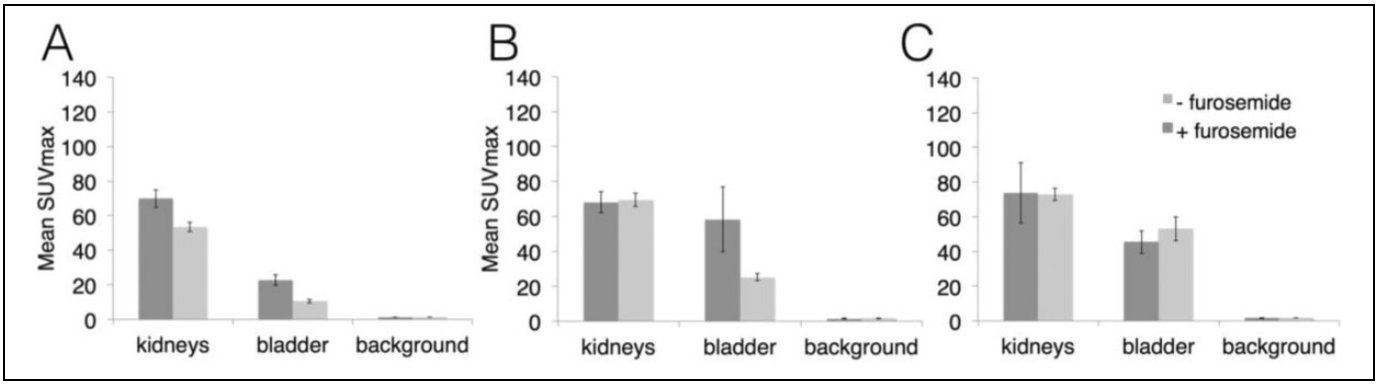

Figure 6. Mean SUVmax measured at kidneys and bladder without (−) and with (+) furosemide administration by scatter correction algorithm: non-time-of-flight (TOF; A), standard TOF (B), and improved TOF (C). Despite overall lower scatter severity, mean SUVmax was at least as high with improved TOF as with non-TOF and standard TOF. Error bars = standard error.

improved TOF groups with similar minimal background uptake, despite the difference in scan delay between the groups. As described in the results section, we found a small but statistically significant improvement in scatter severity ratings overall when imaging at 90+ minutes as opposed to under 90 minutes (Table 2).

A recent study also found that a shorter acquisition time per bed of under 180 seconds was associated with increased scatter artifact.[19] In our study, we imaged for 300 seconds per bed position through the pelvis and abdomen and 180 seconds per bed position from the chest through the vertex. In addition, the arms have been observed to interfere with accurate scatter correction,[15,19] and at least 1 study[17] showed decreased lesion detectability with the arms down. Accordingly, the EANM/SNMMI PSMA guidelines recommend imaging with the arms up.[16] In our study, all PET/MRI patients were imaged with their arms down, which did not appear to worsen scatter artifact in the PET/MRI studies.

Increased object-to-background uptake ratio (OBR) has been speculated to play a role in scatter artifact,[14-16] with at least 1 study[22] demonstrating a positive correlation between OBR and halo size. However, another recent study[17] found no correlation between high bladder activity and the occurrence or severity of scatter artifact, and another study[21] found no difference in lesion detection rates with higher OBR. Nevertheless, administering furosemide to decrease OBR in the urinary system prior to imaging is a commonly advocated practice and is discussed (though not unequivocally recommended) in the EANM/SNMMI PSMA guidelines[16] and several recent studies[18,22] One study[8] demonstrated increased image quality with the use of furosemide. However, furosemide administration is not entirely without risks. Patients may experience an allergic reaction, an adverse drug reaction, or urinary urgency, particularly in the setting of benign prostatic hyperplasia, a common condition in this patient population which can result in difficulty voiding and incomplete voiding. The latter problem could theoretically be avoided by Foley catheterization, but this carries the additional risk of urethral injury and infection. In our study, overall scatter artifact severity was not significantly different when using improved TOF scatter correction, regardless of furosemide administration. The results of our study suggest that furosemide may be useful for scanners employing non-TOF and standard TOF scatter correction but may not be necessary when an improved TOF algorithm is used. This suggests that despite many contributing factors, the key determinant of the presence or absence of scatter artifact is likely the scatter correction algorithm itself. The role of scatter correction algorithm in reducing halo artifact and improving image quality is discussed in several recent studies.[12-14,16-18,23] The TOF is known to produce improved target to noise ratios and subjective image quality[7] and to produce less scatter artifact (although not eliminate it entirely).[15] Additional modifications specifically for Ga-68, including prompt γ correction[13,14,19] and tail fitting modifications,[13,15,19] have been shown to further improve image quality. By demonstrating decreased scatter artifact severity using an improved TOF algorithm, our study is complementary to these other recent studies.

Limitations

A possible confounding factor in our study was the difference between the study groups in delay between radiotracer administration and scan start time. While non-TOF and standard TOF scan delays were similar with a mean of 62.1 and 63.1 minutes, mean improved TOF scan delay was 82.8 minutes. Thus, it is slightly less clear whether the improvement in scatter demonstrated by the improved TOF scatter correction was entirely due to the algorithm itself and not also a longer scan delay. However, as discussed earlier, renal and bladder SUVmax were similar on both standard TOF and improved TOF, despite improved scatter with improved TOF.

Another limitation is the lack of internal controls. A more direct comparison between scatter reduction algorithms would have involved reconstructing the same data sets with and without TOF, as well as with and without improved TOF scatter correction, rather than scanning different patients using the different algorithms. However, this was a retrospective study,

and the overall patient characteristics did not vary widely between the groups.

In addition, furosemide administration was not randomized, which may introduce and element of bias. The reasons patients did not receive furosemide included allergy, hypotension, patient refusal, and technical/nursing error. However, Table 1 demonstrates that the groups who received furosemide were similar to those who did not receive furosemide.

Conclusion

Both furosemide and scatter correction algorithm type play a role in reducing scatter in PSMA PET. Improved TOF scatter correction resulted in the lowest scatter artifact severity and almost no severe scatter artifact, regardless of furosemide administration. Furosemide administration was associated with lower scatter severity when using non-TOF and standard TOF scatter correction.

Declaration of Conflicting Interests

The author(s) declared no potential conflicts of interest with respect to the research, authorship, and/or publication of this article.

Funding

The author(s) received no financial support for the research, authorship, and/or publication of this article.

ORCID iD

Courtney Lawhn-Heath, MD https://orcid.org/0000-0002-1088-3463
David E. Korenchan, PhD https://orcid.org/0000-0001-6152-5896

Supplemental Material

Supplemental material for this article is available online.

References

1. Afshar-Oromieh A, Malcher A, Eder M, et al. PET imaging with a Ga-68-labelled PSMA ligand for the diagnosis of prostate cancer: biodistribution in humans and first evaluation of tumour lesions. *Eur J Nucl Med Mol Imaging*. 2012;40(4):486–495.
2. Afshar-Oromieh A, Haberkorn U, Hadaschik B, et al. PET/MRI with a Ga-68-PSMA ligand for the detection of prostate cancer. *Eur J Nucl Med Mol Imaging*. 2013;40(10):1629–1630.
3. Roethke MC, Kuru TH, Afshar-Oromieh A, et al. Hybrid positron emission tomography–magnetic resonance imaging with gallium-68 prostate-specific membrane antigen tracer: a next step for imaging of recurrent prostate cancer—preliminary results. *Eur Urol*. 2013;64(5):862–864.
4. Afshar-Oromieh A, Avtzi E, Giesel FL, et al. The diagnostic value of PET/CT imaging with the Ga-68-labelled PSMA ligand HBED-CC in the diagnosis of recurrent prostate cancer. *Eur J Nucl Med Mol Imaging*. 2014;42(2):197–209.
5. Nayak B, Dogra PN, Naswa N, et al. Diuretic 18F-FDG PET/CT imaging for detection and locoregional staging of urinary bladder cancer: prospective evaluation of a novel technique. *Eur J Nucl Med Mol Imaging*. 2012;40(3):386–393.
6. Surti S, Karp JS. Advances in time-of-flight PET. *Phys Med*. 2016;32(1):12–22. Elsevier.
7. Karp JS, Surti S, Daube-Witherspoon ME, Muehllehner G. Benefit of time-of-flight in PET: experimental and clinical results. *J Nucl Med*. 2008;49(3):462–470.
8. Derlin T, Weiberg D, Klot von C, et al. Ga-68-PSMA I&T PET/CT for assessment of prostate cancer: evaluation of image quality after forced diuresis and delayed imaging. *Eur Radiol*. 2016;26(12):4345–4353.
9. Kamel EM, Jichlinski P, Prior JO, et al. Forced diuresis improves the diagnostic accuracy of 18F-FDG PET in abdominopelvic malignancies. *J Nucl Med*. 2006;47(11):1803–1807.
10. Nanabala R, Anees MK, Sasikumar A, Joy A, Pillai MR. Preparation of Ga-68-PSMA-11 for PET-CT imaging using a manual synthesis module and organic matrix based 68Ge/Ga-68 generator. *Nucl Med Biol*. 2016;43(8):463–469.
11. Wollenweber SD, Ambwani S, Lonn AHR, et al. Comparison of=4-Class and continuous fat/water methods for whole-body, MR-based PET attenuation correction. *IEEE Transactions on Nuclear Science*. 2013;60(5):3391–3398.
12. Deller T, Khalighi MM, Lantos J, Gulaka P, Iagaru A. Evaluation of improved scatter correction with highly targeted Ga-68-labeled radiopharmaceuticals. *J Nucl Med*. 2016;57(supplement 2):481.
13. Wangerin KA, Baratto L, Khalighi MM, et al. Clinical Evaluation of 68Ga-PSMA-11 and 68Ga-RM2 PET Images Reconstructed With an Improved Scatter Correction Algorithm. *Am J Roentgenol*. 2018;211(3):655–660.
14. Afshar-Oromieh A, Haberkorn U, Schlemmer HP, et al. Comparison of PET/CT and PET/MRI hybrid systems using a Ga-68-labelled PSMA ligand for the diagnosis of recurrent prostate cancer: initial experience. *Eur J Nucl Med Mol Imaging*. 2013;41(5):887–897.
15. Heusser T, Mann P, Rank CM, et al. Investigation of the halo-artifact in Ga-68-PSMA-11-PET/MRI. *PLoS ONE*. 2017;12(8):e0183329. doi: 10.1371/journal.pone.0183329.
16. Fendler WP, Eiber M, Beheshti M, et al. Ga-68-PSMA PET/CT: Joint EANM and SNMMI procedure guideline for prostate cancer imaging: version 1.0. *Eur J Nucl Med Mol Imaging*. 2017;44(6):1014–1024.
17. Afshar-Oromieh A, Wolf M, Haberkorn U, et al. Effects of arm truncation on the appearance of the halo artifact in Ga-68-PSMA-11 (HBED-CC) PET/MRI. *Eur J Nucl Med Mol Imaging*. 2017;44(10):1636–1646.
18. Afshar-Oromieh A, Sattler LP, Mier W, et al. The clinical impact of additional late PET/CT imaging with Ga-68-PSMA-11 (HBED-CC) in the diagnosis of prostate cancer. *J Nucl Med*. 2017;58(5):750–755.
19. Noto B, Büther F, Springe der KA, et al. Impact of PET acquisition durations on image quality and lesion detectability in whole-body Ga-68-PSMA PET-MRI. *EJNMMI Res*. 2017;7(1):12.
20. Domachevsky L, Bernstine H, Goldberg N, et al. Early Ga-68-PSMA PET/MRI acquisition: assessment of lesion detectability and PET metrics in patients with prostate cancer undergoing

same-day late PET/CT. *Clin Radiol*. 2017. doi: 10.1016/j.crad.2017.06.116.

21. Schmuck S, Nordlohne S, Klot CA, et al. Comparison of standard and delayed imaging to improve the detection rate of Ga-68-PSMA I&T PET/CT in patients with biochemical recurrence or prostate-specific antigen persistence after primary therapy for prostate cancer. *Eur J Nucl Med Mol Imaging*. 2017;44(6):960–968.
22. Freitag MT, Radtke JP, Afshar-Oromieh A, et al. Local recurrence of prostate cancer after radical prostatectomy is at risk to be missed in Ga-68-PSMA-11-PET of PET/CT and PET/MRI: comparison with mpMRI integrated in simultaneous PET/MRI. *Eur J Nucl Med Mol Imaging*. 2017;44(5):776–787.
23. Rezaei A, Salvo K, Vahle T, et al. Plane-dependent ML scatter scaling: 3D extension of the 2D simulated single scatter (SSS) estimate. *Phys Med Biol*. 2017;62(16):6515–6531.